Frontiers of Environmental Science & Engineering
2025, 19(12): 166 https://doi.org/10.1007/s11783-025-2086-4

RESEARCH ARTICLE

Substrate competition over 320 days maintains extracellular electron transfer and parallel genomic evolution in *Shewanella oneidensis* MR-1

Biyi Zhao[1,2], Wei Chen[1,2], Geng Chen[1], Feng Zhao[2,3], Yong Xiao ✉ [1,2,4]

1. State Key Laboratory of Regional and Urban Ecology, Institute of Urban Environment, Chinese Academy of Sciences, Xiamen 361021, China
2. University of Chinese Academy of Sciences, Beijing 100049, China
3. State Key Laboratory of Advanced Environmental Technology, Institute of Urban Environment, Chinese Academy of Sciences, Xiamen 361021, China
4. Xiamen Key Laboratory of Physical Environment, Institute of Urban Environment, Xiamen 361021, China

HIGHLIGHTS

- *Shewanella oneidensis* MR-1 maintained extracellular electron transfer after 320 d.
- Ferrihydrite respiration aided *S. oneidensis* MR-1 survival under competition.
- Oxygen cultivation enhanced *S. oneidensis* MR-1's adaptation to oxygen.
- Shared mutations (83.96%) revealed cross-environmental parallel evolution.
- Metabolic efficiency was a key strategy in coculture competition.

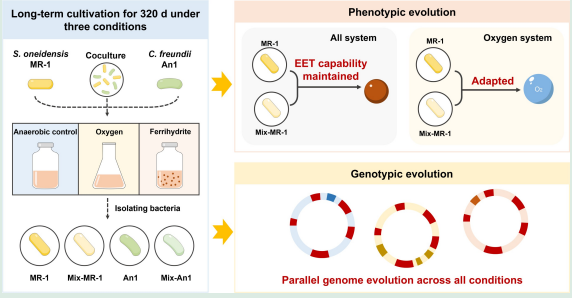

ABSTRACT: Electroactive microorganisms are integral to biogeochemical cycles through extracellular electron transfer and have potential applications in environmental remediation. However, their long-term competitive interactions and evolutionary dynamics with non-electroactive microorganisms remain poorly understood. In this study, we conducted a 320-day cultivation experiment in which monocultures of the electroactive *Shewanella oneidensis* MR-1, the non-electroactive *Citrobacter freundii* An1, and their cocultures were compared under three single electron acceptor conditions: anaerobic (no exogenous electron acceptor), ferrihydrite, or oxygen. After 320 d, *S. oneidensis* MR-1 presented the highest relative abundance of 30.94% ± 0.74% in the ferrihydrite cocultures. *S. oneidensis* MR-1 maintained ferrihydrite reduction capacity after cultivation under all three conditions, indicating the long-term stability of its extracellular electron transfer. Moreover, no other phenotypic evolution was observed in *S. oneidensis* MR-1 after ferrihydrite or anaerobic cultivation. In contrast, both monocultured and cocultured *S. oneidensis* MR-1 exhibited enhanced adaptation to oxygen, characterized by increased growth rates, metabolic activity, and reduced cell aggregation. Notably, substrate consumption increased in monocultures but decreased in cocultures, suggesting an optimization of metabolic efficiency in the

✉ Corresponding author. E-mail: yxiao@iue.ac.cn
Article history: Received 14 May 2025, Revised 26 August 2025, Accepted 29 August 2025, Available online 25 September 2025

latter. Genome sequencing revealed mutations in genes associated with cell division, adenosine triphosphate synthesis, lactate metabolism, and flagellar/pilus expression in *S. oneidensis* MR-1. Interestingly, the ferrihydrite-adapted groups also exhibited enhanced adaptation to oxygen. 83.96% of mutations were shared across all culture systems and enriched in environmental signal-sensing pathways, indicating that parallel genomic evolution facilitated cross-environmental adaptation. Our findings reveal the ecological evolution of electroactive microorganisms in diverse redox environments and establish a foundation for engineering electroactive communities.

KEYWORDS: Extracellular electron transfer, Electroactive microorganisms, Substrate competition, Evolution, *Shewanella*, *Citrobacter*

1 Introduction

The ability of microorganisms to transfer electrons to solid minerals, electrodes, or other microbes via extracellular electron transfer (EET) is essential for redox cycling of elements such as iron and manganese, as well as for regulating redox interfaces in soil, sediment, and groundwater (Lovley, 1991; Melton et al., 2014; Shi et al., 2016; Yang et al., 2023; Kundu et al., 2025). This process is intrinsically coupled to substrate metabolism, as electroactive microorganisms (EAMs) oxidize organic compounds to obtain both carbon and electrons for respiration and extracellular electron flow (Yu et al., 2019; Qi et al., 2024). Despite this capacity, EET-based microbial electrochemical technologies have shown considerable promise in applications such as environmental remediation, bioenergy production, and synthetic ecology (Logan et al., 2006; Demirbas, 2011). However, the effectiveness of these technologies is often constrained by complex microbial interactions that shape the metabolism and activity of EAMs in natural environments (Rabaey et al., 2007; Koch et al., 2018; Zhang et al., 2020). Among these interactions, interspecific competition, one of the most common ecological relationships in microbial ecosystems (Foster and Bell, 2012; Mitri and Foster, 2013; Palmer and Foster, 2022), drives community succession and functional evolution through mechanisms such as resource competition and metabolic inhibition (Lawrence et al., 2012; Bailey et al., 2013; Ghoul and Mitri, 2016). Although approximately 100 EAM species have been identified to date (Koch and Harnisch, 2016; Logan et al., 2019), they are vastly outnumbered by the estimated 10^{12} microbial species in natural environments (Locey and Lennon, 2016), potentially intensifying substrate-level competition and ecological stress for EAMs *in situ*. Therefore, elucidating the evolutionary responses of EAMs to interspecific competition is essential for elucidating their ecological niche maintenance strategies and for optimizing functional microbial consortia in electrochemical systems.

Previous studies on the long-term community succession of microbial EAM biofilms under interspecies competition have focused primarily on interactions among EAMs themselves (Yan et al., 2021), often neglecting the competitive pressure exerted by non-EAMs (Kundu et al., 2025), which may be more abundant in natural environments. In our recent study, we demonstrated that short-term (7 d) substrate competition from the non-EAM *Citrobacter freundii* An1 enhanced the EET activity of *Shewanella oneidensis* MR-1, suggesting that EAMs can flexibly modulate their electron transfer capacity in response to competition for metabolic substrates (Xiao et al., 2021). However, long-term effects, such as gene expression adaptation and community stability, remain poorly explored. Furthermore, although EAMs are widely applied in anaerobic microbial electrochemical systems, their natural habitats often include aerobic environments, such as wastewater, freshwater, or marine sediments (Chabert et al., 2015), as many EAMs are facultative anaerobes (Koch and Harnisch, 2016). Despite this ecological versatility, the mechanistic basis of EAM evolution under aerobic conditions remains largely unexplored. Investigating the evolutionary dynamics of EAMs under various redox conditions, particularly in the context of interspecies competition, is essential for revealing their broad-spectrum adaptive strategies. Such insights will not only deepen our understanding of EAM ecology but also inform the design of stable, efficient electroactive microbial consortia capable of functioning across diverse and complex electron transfer environments.

In this study, we established three culture systems, namely, no exogenous electron acceptor, ferrihydrite, and oxygen, using lactate as the substrate (Fig. 1(a)). Monocultures of *S. oneidensis* MR-1, *C. freundii* An1, and their cocultures were cultivated for 320 d under three conditions. This experimental design enabled us

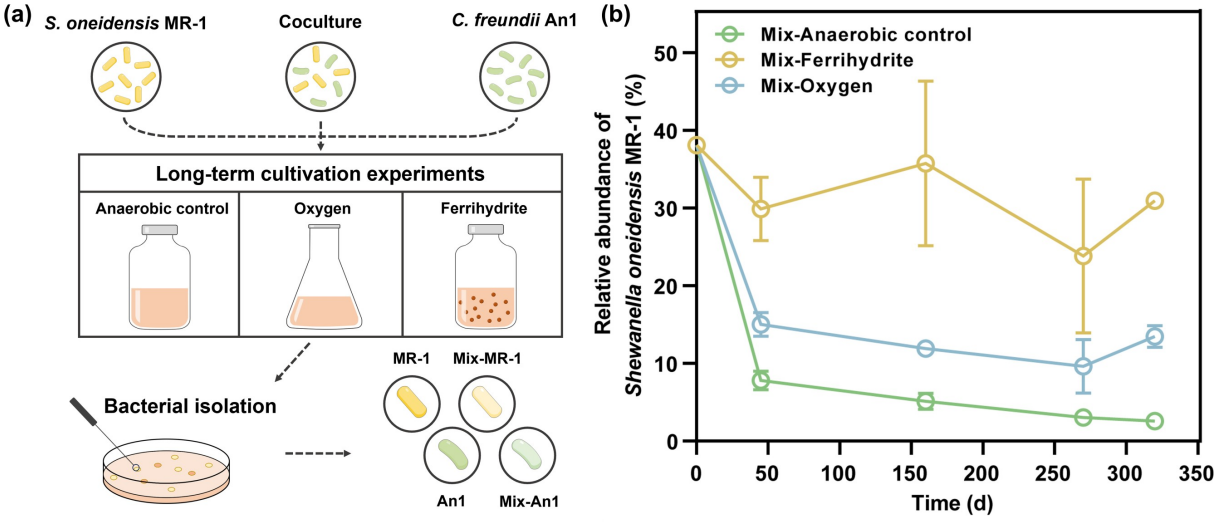

Fig. 1 Framework of the long-term cultivation experiment and relative abundance of *S. oneidensis* MR-1 in coculture groups. (a) *S. oneidensis* MR-1 and *C. freundii* An1 were inoculated into monoculture and coculture groups under three different electron acceptor culture systems: no external electron acceptor (anaerobic control system), oxygen (oxygen system), and ferrihydrite (ferrihydrite system). The initial inoculation ratio in all coculture groups was kept consistent across the three conditions, with three replicates for each group. A minimum of 10 colonies were isolated from each group and pooled into a single test tube for further analysis. The experiment consisted of four groups for each system: monoculture of *S. oneidensis* MR-1 (MR-1 group), monoculture of *C. freundii* An1 (An1 group), coculture of *S. oneidensis* MR-1 (Mix-MR-1 group), and coculture of *C. freundii* An1 (Mix-An1 group). Whole-genome sequencing and associated phenotypic analyses were conducted to explore microbial evolutionary responses to environmental condition and substrate competition. (b) Relative abundance of *S. oneidensis* MR-1 in coculture groups across the different culture systems over time. All groups, except the initial inoculation ratio, were conducted in triplicate.

to investigate long-term microbial interactions at both the ecological and evolutionary levels, including substrate competition between electroactive and non-electroactive species, as well as potential cross-environmental adaptations. We hypothesized that under ferrihydrite condition, *S. oneidensis* MR-1 would maintain or enhance its EET capacity compared to the ancestral strain, whereas its EET capacity would be diminished under oxygen and no exogenous electron acceptor conditions. Furthermore, we anticipated that substrate competition might redirect the evolutionary trajectory of *S. oneidensis* MR-1, affecting both its EET performance and specific strategies for environmental adaptation. By integrating genomic mutation analysis with phenotypic characterization, we aimed to elucidate the mechanisms by which EAMs evolve and adapt under long-term competition across diverse environments.

2 Materials and methods

2.1 Chemicals and materials

Tryptone and yeast extract (FMB grade) were purchased from Sangon Biotech Co., Ltd. (Shanghai, China). NaCl, glycerol, sodium lactate solution (50%–60%), KCl, NH_4Cl, $NaH_2PO_4{\cdot}2H_2O$, $Na_2HPO_4{\cdot}12H_2O$, $MgCl_2{\cdot}6H_2O$, $CaCl_2{\cdot}2H_2O$, KH_2PO_4, Na_2HPO_4, KOH, $Fe(NO_3)_3{\cdot}9H_2O$, hydroxylamine hydrochloride, and 1,10-phenanthroline, all of analytical grade, were purchased from Sinopharm Chemical Reagent Co., Ltd. (Beijing, China). Standard samples for lactate assay were prepared with analytical standard grade L-lactic acid, purchased from Shanghai Aladdin Biochemical Technology Co., Ltd. (Shanghai, China). ATP (adenosine triphosphate) levels were measured using the BacTiter-Glo™ Microbial Cell Viability Assay Kit (Promega, Madison, WI, USA). The SYTO 9/PI Live/Dead Bacterial Double Stain Kit used for cell staining was purchased from Nonin Biological Technology Co., Ltd. (Shanghai, China).

2.2 Bacterial strains and culture systems

We used a previously characterized consortium of *S. oneidensis* MR-1 and *C. freundii* An1 (Xiao et al., 2021). Strains were cultured in Luria-Bertani (LB) medium (pH 7.0) to resuscitate from −80 °C storage. *S. oneidensis* MR-1 and *C. freundii* An1 were cultivated

FSE-25119-ZBY 2025-09-20 12:06:54

in monoculture and coculture for long-term cultivation using a cultivation medium, which was consistent with previous studies (Xiao et al., 2021). The medium for the anaerobic control and ferrihydrite groups were purged with nitrogen gas for 45 min to remove oxygen. No electron acceptors were added to the anaerobic control medium, while the ferrihydrite medium was supplemented with ferrihydrite to a final concentration of 4 mmol/L. Ferrihydrite was synthesized according to a previous study (Zheng et al., 2020). The culture temperature was set at 30 °C, and the flasks were shaken at a speed of 150 r/min.

2.3 Long-term cultivation experiment

On the basis of differences in electron acceptors, the long-term cultivation experiment was divided into three culture systems, each consisting of three treatment groups: a monoculture of *S. oneidensis* MR-1, a monoculture of *C. freundii* An1, and a coculture of both bacteria (Fig. 1(a)). Three replicates were used for each treatment group. To generate mixed groups, ~2.8×10^6 *S. oneidensis* MR-1 and *C. freundii* An1 cells were inoculated into the medium at the beginning of the experiment. Monoculture groups of *S. oneidensis* MR-1 and *C. freundii* An1 were inoculated with the same cell density as the coculture group. The subculturing cycles for the anaerobic control, oxygen, and ferrihydrite systems were approximately 4, 7, and 10 d, respectively, due to differences in growth rates among the systems. In this study, we consider both the 160- and 320-d cultivation periods as long-term, which is consistent with previous studies on microbial evolution where experiments typically span several months (Finkel and Kolter, 1999; Yan et al., 2021; Shen et al., 2024). During long-term cultivation, 1% of the parent cells were inoculated into fresh medium at the end of each cycle.

LB plates (LB medium with 1.5% agar) were used to isolate *S. oneidensis* MR-1 and *C. freundii* An1 from the monoculture and coculture groups after 160 and 320 d. The color of the colonies differentiated the strains, with pink indicating *S. oneidensis* MR-1 and cream indicating *C. freundii* An1. At least three independent colonies were selected and inoculated into LB medium for 24 h. The bacterial suspension was mixed with an equal volume of 50% sterile glycerol and stored at −80 °C for further analysis. The bacterial suspension was additionally identified by 16S rRNA gene sequencing to confirm the purity of the final population. The names of the *S. oneidensis* MR-1 and *C. freundii* An1 samples isolated from the monoculture and coculture groups in different electron acceptor systems are shown in Supplementary material Table S1. The precultured strains of *S. oneidensis* MR-1 and *C. freundii* An1 were designated ancestral strains and referred to as 0 d-MR-1 and 0d-An1, respectively.

2.4 Analysis of bacterial communities

Coculture samples were collected at 0, 45, 160, 270, and 320 d from the three culture systems were centrifuged at 12000 × *g* for 5 min to collect the cells. 16S rRNA gene sequencing was performed on the Illumina 300 platform by Biomarker Technologies Corporation (Beijing, China).

2.5 Whole genome resequencing and bioinformatics analysis

We sequenced the genomes of 73 bacterial samples on the Illumina 300 platform (Biomarker Technologies Corporation, Beijing, China), including: 1) two ancestral populations (0 d-MR-1 and 0d-An1); 2) 36 samples after 160 d of cultivation; and 3) 35 samples after 320 d of cultivation, with the 320 d-Oxygen-Mix-MR-1_1 sample missing. After DNA extraction, the quality of the genomic DNA was assessed using a NanoDrop spectrophotometer (NanoDrop 2000, Thermo, USA) and a Qubit fluorometer (Invitrogen Qubit3.0, Thermo, Singapore). DNA libraries (~350 bp) were prepared following standard protocols and sequenced with 150-bp paired-end reads on an Illumina NovaSeq 6000 platform by Biomarker Technologies (Beijing, China). Clean reads were aligned to the reference genomes of *S. oneidensis* MR-1 and *C. freundii* An1 using BWA-MEM2 v2.2. Redundant or low-quality alignments were removed using SAMtools v1.9. Bioinformatics analysis was performed as described in our previous study (Xiao et al., 2019). Specifically, variant calling was performed using the GATK toolkit to identify single-nucleotide polymorphisms (SNPs) on the basis of comparisons with the corresponding ancestral genomes. Bacterial genome sequencing data are available through the National Microbiology Data Center (NMDC) with accession numbers NMDC10019703 and NMDC10019704.

2.6 Growth curves

A growth curve experiment was conducted to compare the growth characteristics of the ancestral and evolved populations. After activation in LB medium for 16 h at

FSE-25119-ZBY 2025-09-20 12:06:54

30 °C and 150 r/min, the bacterial mixture was inoculated into the corresponding cultivation medium, with an initial optical density at 600 nm (OD_{600}) of approximately 0.02. The growth curves were measured for at least 24 h, and at least six optical density readings were recorded. The maximum optical density ($Max(OD_{600})$) for each sample was defined as the highest value in its growth curve.

2.7 Lactate assay

Our previous study revealed that *S. oneidensis* MR-1 and *C. freundii* An1 primarily metabolize lactate to produce acetate (Xiao et al., 2021). The bacterial samples were resuscitated in LB medium for 16 h at 30 °C and 150 r/min. The bacterial mixture was collected by centrifugation at 5000 × *g* for 10 min, washed twice with 0.85% NaCl, and then inoculated into the ammonium mineral salts (AMS) medium (OD_{600} = 0.5) for continuous culture at 30 °C and 150 r/min. In addition to 5 mmol/L sodium lactate, ASM medium (per liter) contained 0.202 g $MgCl_2 \cdot 6H_2O$, 0.140 g $CaCl_2 \cdot 2H_2O$, 0.214 g NH_4Cl, 0.272 g KH_2PO_4, 0.284 g Na_2HPO_4, and 1 mL of trace element solution was prepared as described in a previous study (Lin et al., 2021). The anaerobic control and ferrihydrite culture systems were purged with nitrogen gas for 45 min to remove oxygen. In the ferrihydrite system, ferrihydrite was added to a final concentration of 4 mmol/L. The medium (1 mL) from each group was collected and centrifuged at 12000 × *g* for 5 min to pellet the cells. The resulting supernatant was then filtered through a 0.22 μm membrane filter to remove bacteria. The liquid samples were acidified to a pH in the range of 1–3 by the addition of sulfuric acid prior to volatile fatty acid analysis. The composition and concentration of volatile fatty acids were measured by a high-performance liquid chromatograph (LC-20A, Shimadzu, Japan) equipped with a strong cation-exchange column (Aminex HPX-87H, Bio-rad, USA).

2.8 Ferrihydrite reduction assay

The culturing procedure for culturing strains of *S. oneidensis* MR-1 and *C. freundii* An1 was the same as that described in Section 2.5 (Lactate assay). Briefly, the strains were cultured in LB medium for 16 h, collected by centrifugation at 5000 × *g* for 10 min, washed twice with 0.85% NaCl, and then transferred to 70 mL of ASM medium containing 4 mmol/L ferrihydrite, with an initial OD_{600} of 0.5 for the bacteria. The culture was incubated continuously at 30 °C and 150 r/min for 10 d, and 0.5 mL of bacterial suspension containing ferrihydrite was collected every two days. The total Fe and Fe(II) concentrations were quantified using the phenanthroline method (Zheng et al., 2020; Lin et al., 2021), and the iron reduction rate was calculated as the ratio of the Fe(II) concentration to the total Fe concentration measured on the same day.

2.9 ATP assay

ATP levels were measured using a firefly luciferase-based ATP assay kit (Yang et al., 2020). The bacterial samples of *S. oneidensis* MR-1 were resuscitated in LB medium for 16 h, inoculated into cultivation medium (OD_{600} = 0.02) and cultured for 4 h under aerobic condition. The bacterial mixture (1 mL) was centrifuged at 13000 × *g* for 5 min, and after the supernatant was removed, the bacteria were resuspended in 1 mL of 0.85% NaCl. For the ATP assay, working dilutions (50 μL) and resuspension mixtures (50 μL) were sequen-tially added to white 96-well cell culture plates and mixed. Luminance in each well was measured using an enzyme marker (Spark, Tecan, Austria). The standard curve was generated using the same method, with the bacterial suspension replaced with ATP standard solutions. The protein concentration was determined by the Bradford method. The ATP concentration was divided by the protein concentration of the same sample to obtain the concentration of ATP per milligram of protein.

2.10 Bacterial morphology

The samples of *S. oneidensis* MR-1 were resuscitated in LB medium for 16 h, washed twice with 0.85% NaCl, and then inoculated into cultivation medium (OD_{600} = 0.02) for 24 h under aerobic condition. To preserve the original bacterial morphology, 90 μL of the cultured bacterial suspension was directly dispersed into 10 μL of fluorescent dye solution (SYTO9, 50 mmol/L; PI, 50 mmol/L) without centrifugation or washing. The mixture was incubated at 4 °C for 15 min for cell staining. After staining, 3 μL of the solution was placed on a glass slide for observation of bacterial morphology using an inverted fluorescence microscope (IX71, Olympus, Japan).

3 Results

3.1 Ferrihydrite promotes the survival of *S. oneidensis* MR-1 in microbial communities

Microorganisms can exhibit varying growth abilities and trends across different environments. To investigate

FSE-25119-ZBY 2025-09-20 12:06:54

this, we measured the variation curves of viable bacterial concentrations of *S. oneidensis* MR-1 and *C. freundii* An1 under three conditions: without any electron acceptor (designated the anaerobic control group), with oxygen (designated the oxygen group), and with ferrihydrite (designated the ferrihydrite group) (Fig. S1). In all three groups, the viable bacterial concentration of *C. freundii* An1 consistently increased and remained higher than that of *S. oneidensis* MR-1, indicating a growth advantage for *C. freundii* An1 in these groups. In the anaerobic control group, the viable concentration of *S. oneidensis* MR-1 decreased, suggesting limited growth. However, in both the oxygen and ferrihydrite groups, *S. oneidensis* MR-1 substantially increased, with its maximum concentration in the oxygen group nearly two orders of magnitude greater than that in the ferrihydrite group. To explore further, we established monoculture and coculture groups of *S. oneidensis* MR-1 and *C. freundii* An1 across the three culture groups for long-term cultivation experiments lasting up to 320 d (Fig. 1(a)).

To investigate the impact of electron acceptors on community composition, the relative abundance of *S. oneidensis* MR-1 in coculture groups subjected to long-term cultivation under three conditions was assessed at 0, 45, 160, and 320 d using high-throughput sequencing (Fig. 1(b)). Over 320 d, the relative abundance of *S. oneidensis* MR-1 decreased in all the groups, indicating that *C. freundii* An1 consistently dominated. The relative abundance of *S. oneidensis* MR-1 was the highest in the Ferrihydrite-Mix group, followed by the Oxygen-Mix group, and the lowest in the Anaerobic control-Mix group. By the end of the experiment, the relative abundances of *S. oneidensis* MR-1 in the Ferrihydrite-Mix group, Oxygen-Mix group and Anaerobic control-Mix group were 30.94% ± 0.74%, 13.47% ± 1.40%, and 2.57% ± 0.10%, representing decreases of 18.80%, 64.64%, and 93.25%, respectively, from the initial levels. A similar trend was observed during the 160- and 320-d incubation periods, where *S. oneidensis* MR-1 was more abundant in the Ferrihydrite-Mix group than in the other two groups (Fig. S2). These findings indicated that ferrihydrite enhanced the survival of *S. oneidensis* MR-1 in substrate-competitive environments.

3.2 Long-term cultivation did not affect the EET capacity of *S. oneidensis* MR-1

S. oneidensis MR-1 can reduce Fe(III) to Fe(II) via the EET process; therefore, we measured the Fe(III) reduction curve to compare the EET capacity of ancestral (0 d-MR-1) and long-term-cultivated *S. oneidensis* MR-1. Compared with the 0 d-MR-1 group, the ferrihydrite-adapted *S. oneidensis* MR-1 group presented higher conversion rates on days 2 and 4 (Fig. 2(a)). However, no significant increase in the final Fe(III) conversion rates was observed (Fig. S3). Additionally, the lack of differences in final conversion rates between the monoculture and coculture groups suggest that *C. freundii* An1 had no notable effect on the Fe(III) reduction capacity of *S. oneidensis* MR-1. Thus, long-term ferrihydrite cultivation did not significantly affect EET capacity.

The Fe(III) reduction curve of oxygen-adapted *S. oneidensis* MR-1 also revealed differences in the Fe(III) conversion rates on days 2 and 4 (Fig. 2(b)). However, its final Fe(III) conversion did not substantially differ from that of the 0 d-MR-1 group (Fig. S4). Similarly, the Fe(III) reduction (Fig. 2(c)) and final Fe(III) conversion (Fig. S5) of the anaerobic-adapted *S. oneidensis* MR-1 were not substantially different from

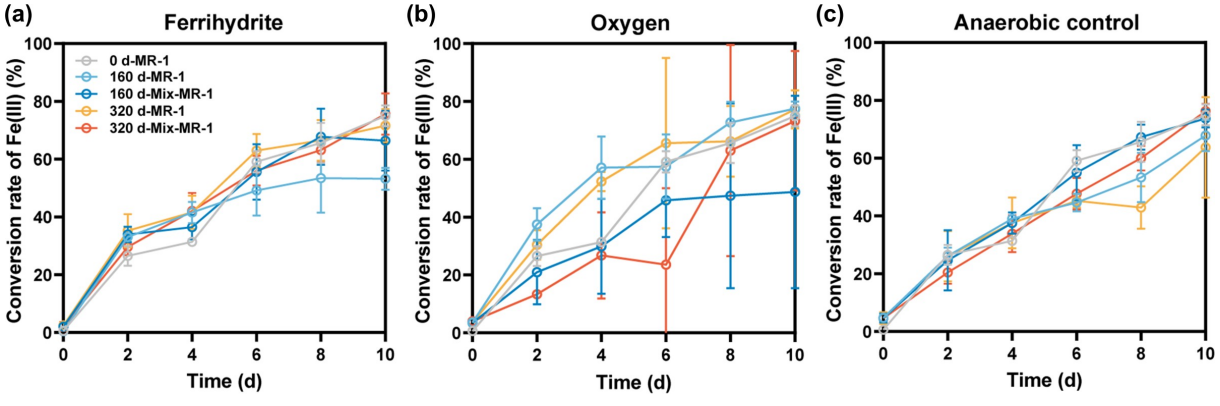

Fig. 2 Long-term cultivation in all three systems did not significantly affect the Fe(III) reduction capacity of *S. oneidensis* MR-1. (a) Ferrihydrite-adapted groups. (b) Oxygen-adapted groups. (c) Anaerobic-adapted groups. In all three graphs, the 0 d-MR-1 group represents the ancestral strain assay, with consistent experiment data.

FSE-25119-ZBY 2025-09-20 12:06:54

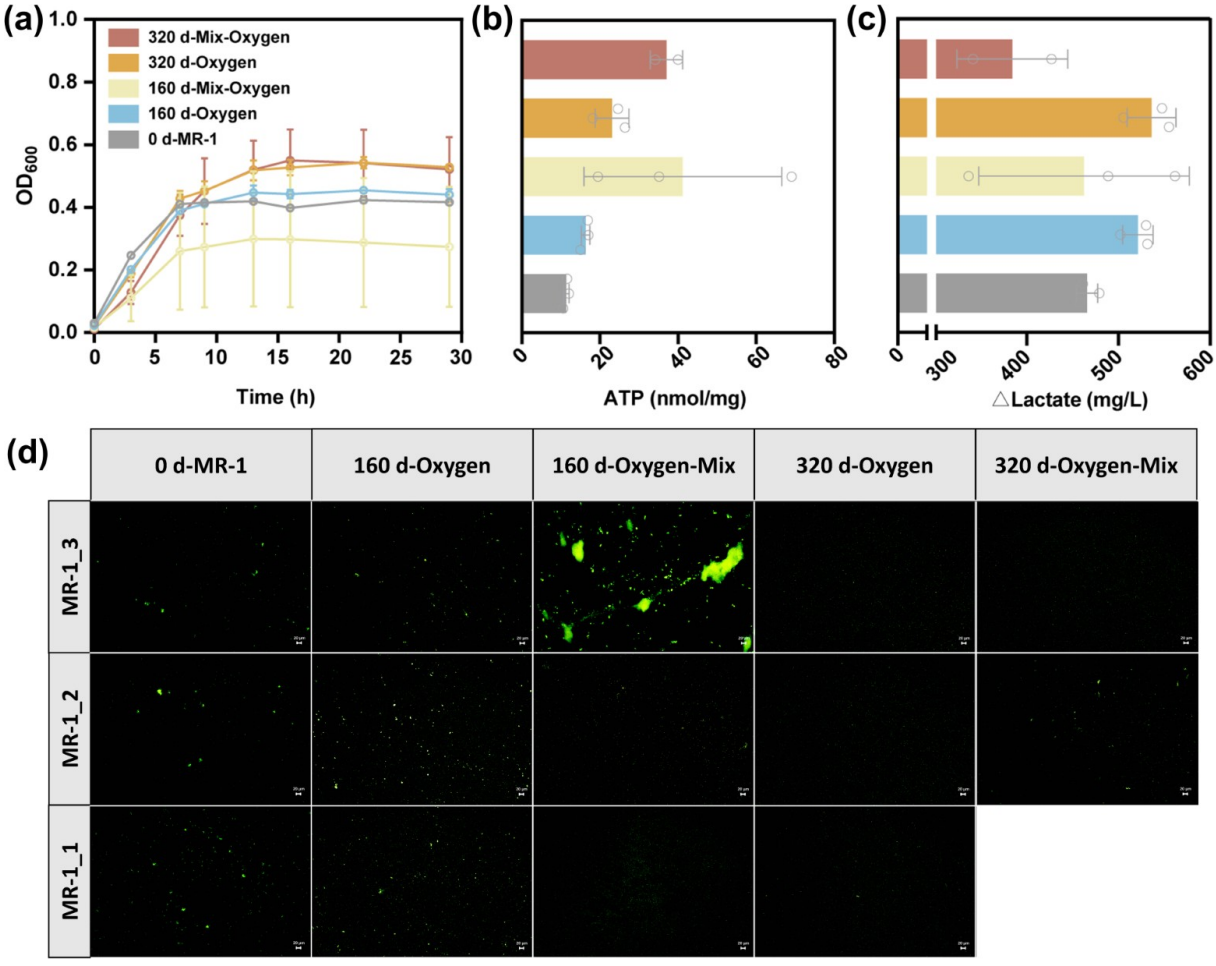

Fig. 3 Long-term oxygen cultivation enhanced the adaptation of *S. oneidensis* MR-1 to oxygen. (a) Growth curves of ancestral and all oxygen-adapted groups after 28 h of cultivation with oxygen. 160 and 320 d represent the cultivation durations, Mix-MR-1 refers to the coculture groups, MR-1 refers to the monoculture groups, and 0d-MR-1 indicates the ancestral *S. oneidensis* MR-1. (b) ATP levels of ancestral and all oxygen-adapted groups after 4 h of cultivation with oxygen. (c) Lactate consumption of ancestral and all oxygen-adapted groups under oxygen condition. (d) Distribution morphology of ancestral and all oxygen-adapted groups after 24 h of cultivation with oxygen. White box indicates missing sample.

those of the 0d-MR-1 group. These results suggested that long-term cultivation with oxygen or without an electron acceptor did not alter the EET capacity of *S. oneidensis* MR-1.

Furthermore, no other phenotypic evolution was observed in ferrihydrite- or anaerobic-adapted *S. oneidensis* MR-1. In the anaerobic-adapted group, the maximum optical density Max(OD_{600}) of the bacterial growth curves did not exceed 0.08 (Fig. S6), indicating limited growth without electron acceptors. Lactate consumption did not substantially differ between all the anaerobic-adapted groups and the 0 d-MR-1 group (Fig. S7(a)), suggesting that long-term cultivation had a minimal effect on growth or metabolism without electron acceptors. Similarly, lactate consumption under ferrihydrite condition remained unchanged compared with that in the 0 d-MR-1 group (Fig. S7(b)).

3.3 Long-term oxygen cultivation promoted the growth and metabolism of *S. oneidensis* MR-1 with oxygen

To assess the oxygen adaptation of *S. oneidensis* MR-1 following long-term oxygen cultivation, we measured the growth curves and Max(OD_{600}) values of both the ancestral strain and all the oxygen-adapted groups. The growth curves revealed that after 10 h, the OD_{600} values of 320 d-Oxygen-MR-1 and 320 d-Oxygen-Mix-MR-1 were greater than that of 0 d-MR-1, whereas the difference between 160 d-Oxygen-MR-1 and 0 d-MR-1 was minimal (Fig. 3(a)). The growth curve differences

FSE-25119-ZBY 2025-09-20 12:06:54

between replicate samples of the 160 d-Oxygen-Mix-MR-1 and 320 d-Oxygen-MR-1 groups may be attributed to substrate competition from *C. freundii* An1 (Aristide and Morlon, 2019). The Max(OD_{600}) values for the 320 d-Oxygen-MR-1 (0.543) and 320 d-Oxygen-Mix-MR-1 (0.550) groups were both higher than that of the 0d-MR-1 group, by 28.29% and 30.02%, respectively (Fig. S8). These results demonstrated that long-term oxygen cultivation increased the growth capacity of *S. oneidensis* MR-1 under oxygen condition in both the monoculture and coculture groups, whereas substrate competition had a limited effect on its growth phenotype.

ATP is the direct source of energy required for metabolism and serves as an indicator of bacterial metabolic activity. To assess the metabolic activity of *S. oneidensis* MR-1, we measured ATP levels after 4 h of incubation under oxygen condition (Fig. 3(b)). Compared with those in the 0 d-MR-1 group, ATP levels were increased in all the oxygen-adapted groups. In the coculture groups, the ATP levels of the 160d-Oxygen-Mix-MR-1 and 320 d-Oxygen-Mix-MR-1 groups increased by approximately 262% and 226%, respectively, relative to those of the 0d-MR-1 group. Additionally, the ATP levels in the coculture groups were greater than those in the monoculture groups at the same cultivation times, with a 152% increase after 160 d and a 60% increase after 320 d. These findings suggested that long-term oxygen cultivation enhanced the metabolic activity of *S. oneidensis* MR-1, while substrate competition from *C. freundii* An1 further amplified the activity under oxygen condition.

The lactate consumption of all the oxygen-adapted groups was measured to compare their substrate utilization abilities (Fig. 3(c)). Compared with that of 0d-MR-1, the lactate consumption of 160 d-Oxygen-MR-1 and 320 d-Oxygen-MR-1 increased by 11.87% and 15.04%, respectively, under oxygen condition, indicating that long-term oxygen cultivation increased the substrate consumption capacity of *S. oneidensis* MR-1 in monocultures. However, substrate consumption in the two coculture groups was lower than that in the 0 d-MR-1 group. These results suggested that *S. oneidensis* MR-1 may employ different metabolic evolutionary strategies in the monoculture and coculture groups.

Furthermore, bacterial aggregates were observed in the 160d-Oxygen-Mix-MR-1_3 sample (Fig. S9), suggesting the potential emergence of an aggregation phenotype during long-term oxygen cultivation. Microscopy imaging was used to observe the stained *S. oneidensis* MR-1 cells, revealing the cell morphology and distribution of bacteria in the 0d-MR-1 and all the oxygen-adapted groups after 24 h of cultivation with oxygen (Fig. 3(d)). The results revealed that aggregates with a maximum area of at least 19200 μm^2 were found only in the 160 d-Oxygen-Mix-MR-1_3 sample. The aggregation phenotype likely resulted from a random genetic mutation and was not retained, as no bacterial aggregates were observed in either the 320 d-Oxygen-MR-1 or 320 d-Oxygen-Mix-MR-1 groups. In contrast, the bacteria in these two groups were more dispersed than those in the 0 d-MR-1 group, with fewer aggregates. These findings indicated that flagella and pili may have played pivotal roles in the adaptive evolution of *S. oneidensis* MR-1 under oxygen condition (Pohlschroder et al., 2011; Nakamura and Minamino, 2019).

3.4 Long-term ferrihydrite cultivation improved the growth of *S. oneidensis* MR-1 under oxygen condition

To explore the potential for trans-environmental adaptation, we characterized the phenotypic traits of all the ferrihydrite-adapted *S. oneidensis* MR-1 groups under oxygen condition. Unexpectedly, the growth curves of all the ferrihydrite-adapted groups, when cultivated under oxygen, exhibited consistently higher OD_{600} values than did the 0d-MR-1 group after 6 h (Fig. 4(a)). The 320 d-Ferrihydrite-Mix-MR-1 group presented the highest Max(OD_{600}), which exceeded that of the 0 d-MR-1 group by 41.57% (Supplementary Fig. 10). The Max(OD_{600}) values of the 160 d-MR-1 and 320 d-MR-1 groups were similar, surpassing those of the 0 d-MR-1 group by 30.47% and 28.27%, respectively. In contrast, the 160d-Mix-MR-1 group presented a smaller increase of 15.51%. These results suggested that, after long-term cultivation with ferrihydrite, *S. oneidensis* MR-1 developed increased cell density and increased growth capacity under oxygen condition.

ATP levels in ancestral and all ferrihydrite-adapted groups were measured after 4 h of cultivation with oxygen. Unlike those in the oxygen-adapted groups, the ATP concentrations in the ferrihydrite-adapted groups were not significantly different from those in the 0d-MR-1 group (Fig. 4(b)). These results suggested that long-term ferrihydrite cultivation did not enhance cellular metabolic activity under oxygen condition. In the 320d group, *S. oneidensis* MR-1 predominantly exhibited a dispersed form, with no obvious aggregates (Fig. 4(c)). Both ferrihydrite- and oxygen-adapted *S. oneidensis* MR-1 underwent phenotypic evolution in terms of growth and motility to adapt to oxygen as an electron acceptor, indicating similar evolutionary mechanisms.

FSE-25119-ZBY 2025-09-20 12:06:54

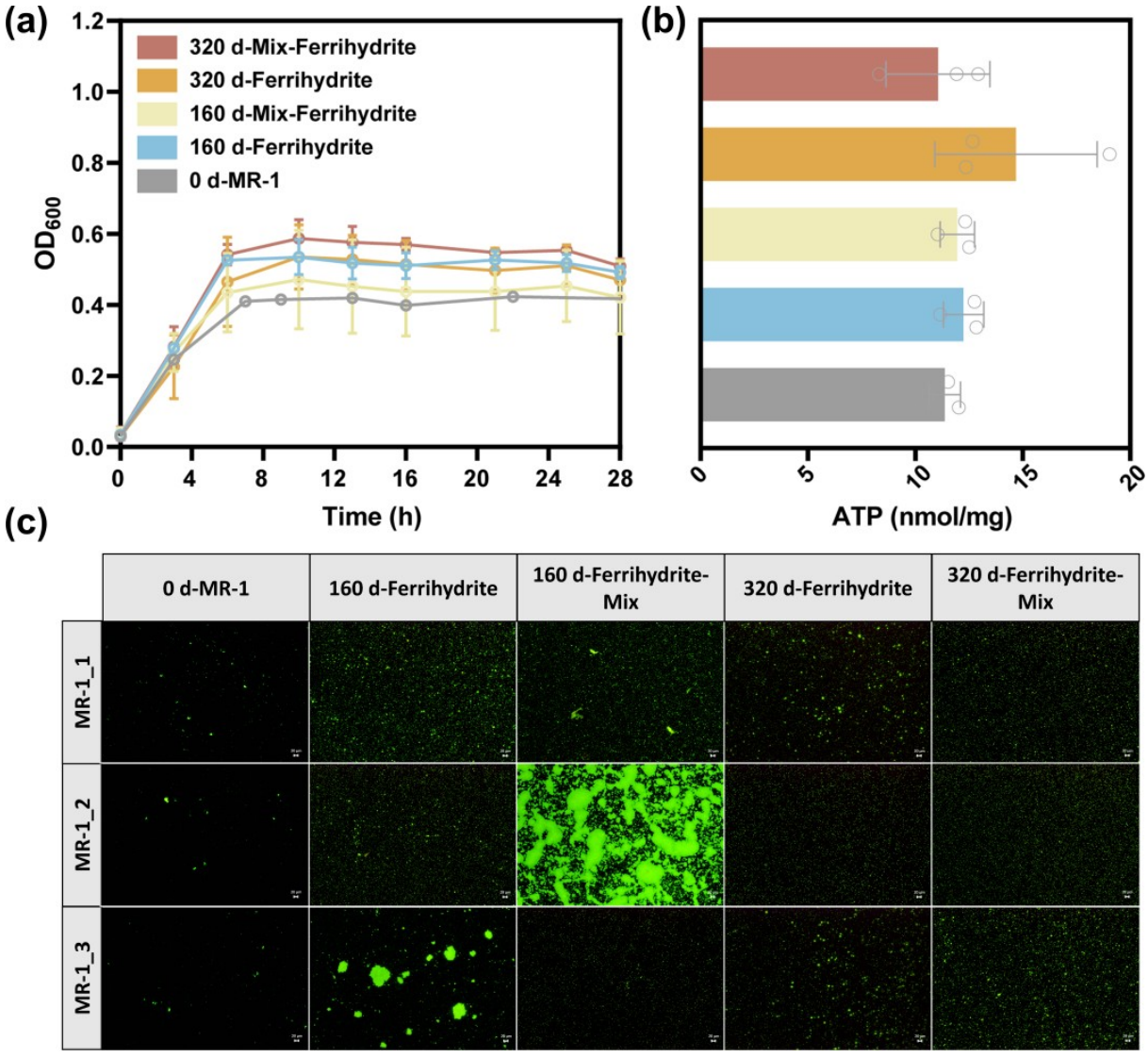

Fig. 4 Long-term ferrihydrite cultivation enhanced the growth of *S. oneidensis* MR-1 under oxygen condition. (a) Growth curves of ancestral and all ferrihydrite-adapted groups after 28 h of cultivation with oxygen. 160 and 320 d represent the cultivation durations, Mix-MR-1 refers to the coculture groups, MR-1 refers to the monoculture groups, and 0d-MR-1 indicates the ancestral *S. oneidensis* MR-1. (b) ATP levels of ancestral and all ferrihydrite-adapted groups after 4 h of cultivation with oxygen. (c) Distribution morphology of ancestral and all ferrihydrite-adapted groups after 24 h of cultivation with oxygen.

3.5 Genetic mutations reveal the evolutionary molecular mechanisms of *S. oneidensis* MR-1 under oxygen and ferrihydrite conditions

SNPs provide insights into the evolutionary strategies employed by bacteria to cope with biotic and abiotic stresses in their environment (Lee et al., 2008). To investigate these strategies, we sequenced the genomes of the ancestral strain and *S. oneidensis* MR-1 populations after 160 and 320 d of long-term cultivation in anaerobic control, oxygen, and ferrihydrite systems. Whole-genome sequencing was performed on 36 samples, and non-synonymous SNPs were identified by comparing all samples to the genome sequence of the ancestral strain (Supplementary Data 1).

In the 160 d groups, the average number of non-synonymous mutations in *S. oneidensis* MR-1 was fewer than 20 (Fig. 5(a)). In contrast, the 320 d groups presented more than 185 mutations, indicating that extended cultivation promoted the accumulation of adaptive mutations in response to environmental stressors. Non-synonymous mutations in the 160 d groups were linked to 90 genes (Fig. S11), whereas mutations in 184 genes were detected in the 320 d

FSE-25119-ZBY 2025-09-20 12:06:54

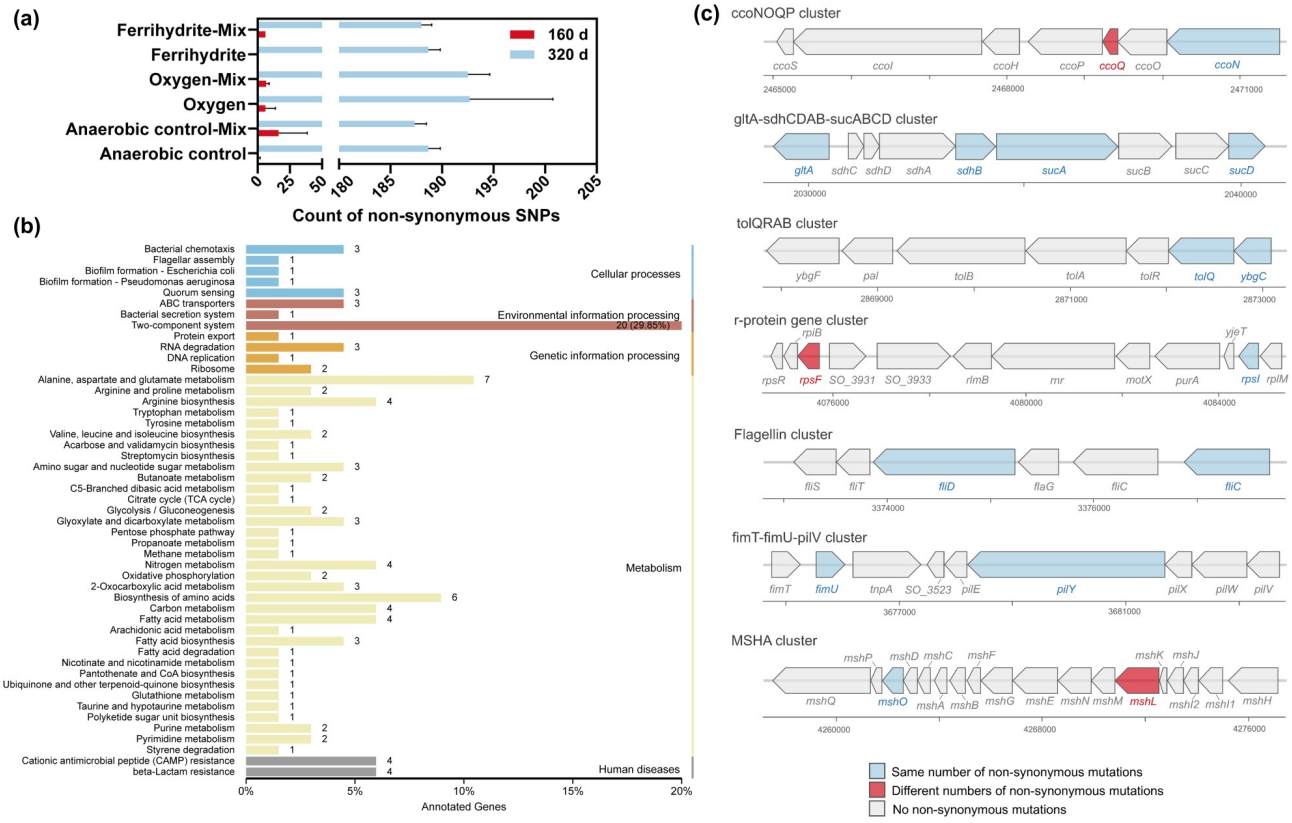

Fig. 5 Molecular mechanisms of *S. oneidensis* MR-1 evolution after 320 d. (a) Number of non-synonymous SNPs in *S. oneidensis* MR-1 after long-term cultivation across three culture systems. Red indicates groups cultivated for 160 d, and blue indicates groups cultivated for 320 d. (b) KEGG pathway analysis of shared non-synonymous SNPs across three culture systems. (c) Key mutated genes and gene clusters potentially contributing to the enhanced adaptation of oxygen- and ferrihydrite-adapted *S. oneidensis* MR-1.

groups (Fig. S12). Given these results, we focused primarily on the non-synonymous mutations that accumulated in the 320 d groups. Notably, 97.8% (n = 88) of the mutated genes in the 160 d groups were also detected in the 320 d groups (Fig. S13). These findings implied that the genetic changes in the 320 d group samples were predominantly extensions of those observed in the 160 d groups.

In the 320 d groups, oxygen-adapted *S. oneidensis* MR-1 groups presented a greater number of non-synonymous mutations compared to ferrihydrite- and anaerobic-adapted groups, regardless of culture type (monoculture or coculture) (Fig. 5(a)). Unexpectedly, 157 shared genes were identified among the 320 d group samples across all culture systems, accounting for 83.96% of the total mutated genes, with 176 non-synonymous SNPs identified (Fig. S12). These results suggested that *S. oneidensis* MR-1 underwent convergent genomic evolution under different conditions, which may partially explain its adaptive evolution to oxygen observed in ferrihydrite-adapted groups.

GO database annotation revealed that 80 shared genes with mutations in the 320 d groups were involved in cellular components, 108 in molecular functions, and 103 in biological processes (Fig. S14). KEGG pathway analysis revealed that 176 non-synonymous SNPs in these shared genes were associated with metabolic pathways, spanning five categories: cellular processes, environmental information processing, genetic information processing, and metabolism and human diseases (Fig. 5(b)). Notably, the largest number of mutated genes (n = 20) were linked to the two-component system pathway. The two-component system plays a critical role in bacterial adaptation to environmental changes, regulating processes such as the stress response, nutrient acquisition, metabolic activity, and chemotaxis (Groisman, 2016; Alvarez and Georgellis, 2023). These pathways likely played a significant role in the long-term cultivation of *S. oneidensis* MR-1.

To elucidate the molecular mechanisms underlying adaptive evolution under oxygen condition, we further analyzed the functions of gene clusters with co-

FSE-25119-ZBY 2025-09-20 12:06:54

mutations (Fig. 5(c)). The *tolQ* and *ybgC* genes, which are part of the Tol–Pal system, are essential for membrane invagination during cell division and influence bacterial growth (Dubuisson et al., 2005; Teleha et al., 2013). Similarly, *zipA*, encoding a cell division protein, plays a critical role in this process (Hale and de Boer, 1997). Mutations in *tolQ*, *ybgC*, and *zipA* likely promoted cell division, contributing to the increased growth rate of *S. oneidensis* MR-1 under oxygen condition. Additionally, non-synonymous mutations in *rpsF*, *rpsG*, and *rpsI*, which regulate ribosomal protein synthesis and cell division, are strongly correlated with bacterial growth rates (Akanuma et al., 2012).

The cbb_3-type cytochrome *c* oxidase, a terminal oxidase in *S. oneidensis* MR-1 under oxygen condition, is critical for oxidative phosphorylation and ATP production (Pinchuk et al., 2010; Yin et al., 2016). Mutations in the *ccoN* gene were observed across all groups, whereas *ccoQ* mutations were exclusive to the oxygen-adapted *S. oneidensis* MR-1 from the coculture groups (Fig. S15). These genetic changes likely contributed to the greater ATP production in the 320 d-Oxygen-Mix-MR-1 group than in the 320 d-Oxygen-MR-1 group (Fig. 3(b)). Additionally, genes associated with the citrate cycle, including *sdhB*, *gltA*, *sucD*, and *sucA* (Li et al., 2006), are linked to aerobic metabolism and ATP synthesis. Mutations in the *llpR* gene, a regulator of lactate utilization in *S. oneidensis* MR-1 (Pinchuk et al., 2009; Brutinel and Gralnick, 2012), may explain the increased lactate consumption observed in the oxygen-adapted *S. oneidensis* MR-1 from the monoculture groups, compared with the 0 d-MR-1 group (Fig. 3(c)).

Non-synonymous mutations in genes associated with flagella and pili, which are essential for bacterial adhesiveness and motility, may impact the microbial growth rate (Zöllner et al., 2017; Gude et al., 2020). Mutations in genes such as *filC*, *filD*, *flgJ*, and *nlpE*, which regulate flagellar assembly and gene expression, likely affect bacterial motility (Tasteyre et al., 2001; Herlihey et al., 2014; Shimizu et al., 2016). Similarly, mutations in *fimU* and *pilY*, which co-encode type IV pili involved in microbial autoaggregation under oxygen condition, were also observed (McLean et al., 2008). Additional mutations in *fimV*, *mshO*, and *mshL*, encoding pili-associated proteins, were linked to pili function, adhesiveness, and twitching motility (Semmler et al., 2000; Sun et al., 2022). These genetic changes may account for the increased maximum growth densities and reduced aggregation observed in the oxygen- and ferrihydrite-adapted groups at 320 d, compared with those of the ancestral strain. Conversely, the 320 d-Oxygen-Mix-MR-1 group presented fewer non-synonymous SNPs in *mshL* and *fimV* than did the 320 d-Oxygen-MR-1 group.

3.6 No phenotypic adaptation occurred in *C. freundii* An1 after long-term cultivation

For the oxygen-adapted groups of *C. freundii* An1, the $Max(OD_{600})$ over 24 h did not significantly differ from that of the ancestral strain (0d-An1 group), with all values remaining at approximately 0.6 (Fig. 6(a)). Similarly, the $Max(OD_{600})$ of the oxygen-adapted groups after 24 h was not significantly different from that of the 0 d-An1 group (Fig. 6(b)). Furthermore, the final Fe(III) conversion rates of the ferrihydrite-adapted groups were comparable to those of the ancestral strain (Fig. 6(c)). These findings suggested that long-term cultivation did not induce phenotypic evolution in *C. freundii* An1 under three electron acceptor conditions.

4 Discussion

Contrary to our initial hypothesis, the EET capacity of *S. oneidensis* MR-1 was not significantly increased under ferrihydrite conditions, nor was diminished under oxygen or anaerobic conditions; instead, it remained stable across all three environments. Furthermore, after 320 d of cultivation, genomic analyses revealed a consistent pattern of parallel evolution across distinct conditions, suggesting that prolonged environmental pressures drove convergent molecular adaptations. This study provides new insights into how electroactive microorganisms evolve under ecological pressures, and reveals evolutionary strategies for genome convergence.

In this study, we confirmed that *S. oneidensis* MR-1 maintained the highest relative abundance under long-term competition with ferrihydrite, compared to the oxygen and no electron acceptors, because of its reliance on EET-driven iron-reducing respiration (Fig. 1(b)). These findings support the view that EET serves as a core survival strategy for EAMs in anaerobic environments enriched with iron oxides (Lovley, 1991). Surprisingly, neither ferrihydrite- nor oxygen-adapted *S. oneidensis* MR-1, whether monocultured or cocultured, presented significantly increased iron-reduction capacity (Figs. 2(a) and 2(b)), and the ferrihydrite-adapted groups lacked increased non-synonymous mutations in EET-related genes (e.g., the cytochrome *c* family). These findings contrast with our previous finding that short-term (7 d) competition with

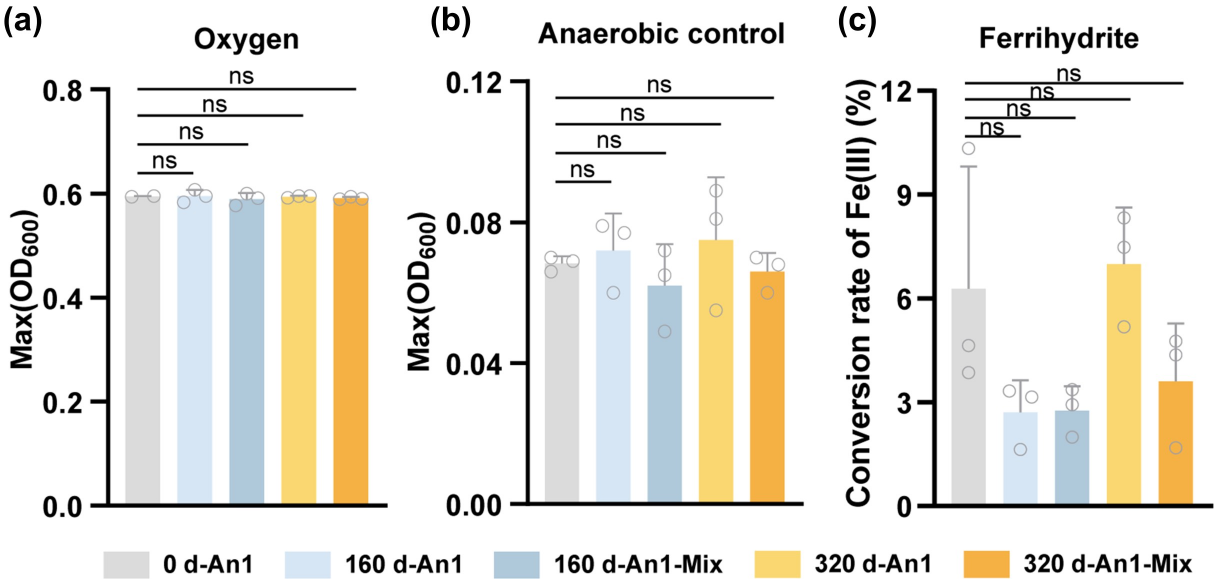

Fig. 6 *C. freundii* An1 exhibited no phenotypic evolution after long-term cultivation under three conditions. (a) Max(OD_{600}) of ancestral and all oxygen-adapted groups over 24 h with oxygen. (b) Max(OD_{600}) of ancestral and all anaerobic-adapted groups over 24 h under anaerobic condition. (c) The final Fe(III) conversion rate of ancestral and all ferrihydrite-adapted groups after 10 d.

C. freundii An1 enhanced EET-related protein expression in *S. oneidensis* MR-1 (Xiao et al., 2021). Collectively, these observations suggest that the EET pathway, which is crucial for iron-reducing respiration, may have already undergone evolutionary optimization, with further adaptation limited by the energetic costs and structural constraints of key proteins (Zaidi et al., 2014; Li et al., 2020). These evolutionary constraints suggest that the functional conservation of EET, a cornerstone of EAM survival, may be a key strategy for microbial communities to maintain stable electron transfer flux.

Our results revealed a novel mechanism by which *S. oneidensis* MR-1 achieves broad-spectrum environmental adaptation through convergent optimization of core regulatory metabolic networks. Whole-genome sequencing revealed a high degree of mutational convergence across all conditions, with 83.96% of the mutations shared among the evolved populations, particularly those enriched in genes encoding two-component regulatory systems (Fig. 5(b)). Notably, the ferrihydrite-adapted populations also exhibited enhanced adaptation to oxygen (Fig. 4), providing additional evidence for parallel genomic evolution. These cross-environment adaptations illustrate how EAMs evolve flexible survival strategies while preserving core EET functionality. As central hubs for environmental sensing and response, mutations in two-component system genes may promote broad signal transduction optimization, enabling *S. oneidensis* MR-1 to rapidly adjust to diverse environmental conditions (Martín-Rodríguez et al., 2022; Alvarez and Georgellis, 2023). This evolutionary strategy likely supports the maintenance of EET functional homeostasis in dynamic habitats such as sediment–water interfaces, while conferring the metabolic flexibility necessary to withstand interspecies competition. The 320-d samples presented a greater number of SNPs than 160-d samples did, which is consistent with the theory that adaptive mutations accumulate progressively under sustained selective pressure (Lenski and Travisano, 1994; Barrick et al., 2009). This finding suggests that achieving cross-environment parallel evolution may require both sufficient evolutionary time and the gradual buildup of mutations.

The evolutionary trajectory of *S. oneidensis* MR-1 under combined selection by oxygen and interspecific competition highlights metabolic efficiency optimization as a key competitive strategy. Both monocultured and cocultured oxygen-adapted populations acquired mutations in genes related to cell division, such as *tolQ* and *rpsF* (Fig. 5(c)), which corresponded with increased maximum growth densities (Fig. 3(a)), suggesting that enhanced proliferative capacity represents a conserved microbial adaptation mechanism (Farshadzadeh et al., 2018; Hu et al., 2024). In addition, mutations in adhesion- and motility-associated genes, such as *flgJ* and *pilY* (Fig. 5(c)), were associated with reduced cell aggregation (Fig. 3(d)), which may have facilitated improved growth under both monoculture

FSE-25119-ZBY 2025-09-20 12:06:54

and coculture conditions (Zöllner et al., 2017; Gude et al., 2020). In the cocultures, the lower frequency of non-synonymous mutations in *mshL* and *fimV* (Fig. 5(c)) indicated the selective retention of motility-related functions, potentially enhancing substrate acquisition under competitive conditions (Moens and Vanderleyden, 1996; Chen et al., 2024).

Notably, cocultured *S. oneidensis* MR-1 populations consumed less lactate yet produced more ATP than monocultured populations did (Figs. 3(b) and 3(c)), indicating an evolutionary shift toward greater metabolic efficiency. In resource-limited environments, such strategies—characterized by reduced substrate uptake coupled with increased energy yield—may provide a fitness advantage over rapid consumption alone. Previous studies have suggested that such metabolic refinement allows microbes to avoid inefficient resource competition by maximizing ATP yield per unit of substrate (Pfeiffer et al., 2001; MacLean, 2008; Pettersen et al., 2020). Our long-term findings demonstrate that these energy-efficient strategies were not transient adaptations but were stably selected through specific genomic changes, highlighting the influence of community structure in shaping evolutionary outcomes. While monocultures favored faster growth through greater resource use, cocultures selected for optimized energy metabolism, driven by sustained interspecies competition. Together, these findings provide direct genomic and physiological evidence that long-term ecological interactions can drive metabolic optimization, offering important insights for the design of robust electroactive microbial consortia.

The observed threshold-dependent phenotypic evolution offers key insights for engineering resilient electroactive communities. This study suggested that microbial phenotypic evolution may occur only when environmental stresses surpass species-specific thresholds. In long-term cultivation experiments, *S. oneidensis* MR-1 exhibited enhanced adaptation to oxygen (Fig. 3), likely due to its rapid aerobic growth (Fig. S1), which may have intensified both intraspecific and interspecific competitive pressures. These pressures could have prompted environmental stress beyond the evolutionary threshold for this species (Hoffmann and Hercus, 2000; Rigato and Fusco, 2020; Venkataram et al., 2020). Understanding these threshold dynamics enables the rational design of microbial consortia in which EAMs sustain stable EET while acquiring beneficial adaptive traits. In contrast, under ferrihydrite and anaerobic conditions, *S. oneidensis* MR-1 exhibited weaker growth (Fig. S1), and the associated stress may have remained below the threshold, resulting in no observable phenotypic evolution (Figs. S6 and S7). Notably, *C. freundii* An1 did not undergo phenotypic evolution under any condition (Fig. 6), despite achieving higher growth density than *S. oneidensis* MR-1 did (Fig. S1), suggesting that the threshold for stress-induced phenotypic evolution varies between species (Moczek et al., 2002). These findings implied that when electroactive microbial communities are constructed, selecting EAMs with lower adaptation thresholds under specific redox conditions could accelerate functional optimization. Moreover, community design should prioritize metabolic interactions that heighten competition or resource limitation, as these interactions can increase evolutionary pressures and promote functional evolution (e.g., increased EET rates or electron donor specificity).

5 Conclusions

This study has offered important insights into the evolutionary adaptation of EAMs to long-term interspecies competition with non-EAMs under various redox conditions. Our results showed that ferrihydrite-dependent EET conferred a competitive advantage to *S. oneidensis* MR-1 in substrate-limited environments, allowing it to maintain a greater relative abundance than the oxygen and anaerobic control groups. After 320 d of cultivation, *S. oneidensis* MR-1 consistently maintained a stable EET capacity, which was unaffected by redox conditions (ferrihydrite or oxygen) or substrate competition. Phenotypic evolution was observed exclusively in oxygen-adapted populations, which presented increased growth rates, elevated metabolic activity, and reduced cell aggregation. Whole-genome sequencing revealed the molecular mechanisms of oxygen adaptation in *S. oneidensis* MR-1 and identified metabolic efficiency optimization as a core competitive strategy. Notably, parallel genomic evolution was evident, with 83.96% of mutations shared across all conditions and enriched in two-component system genes, underscoring their role in broad-spectrum environmental sensing and cross-environmental adaptation. Furthermore, *C. freundii* An1 exhibited no phenotypic evolution under any condition. Collectively, these findings advance our understanding of EAM ecology and offer guidance for engineering resilient electroactive communities in microbial electrochemical systems.

CRediT Authorship Contribution Statement

Biyi Zhao: Writing-review & editing, Writing-original draft, Conceptualization, Investigation, Methodology, Formal analysis,

Visualization, Data curation. **Wei Chen**: Writing-review & editing, Methodology, Formal analysis, Visualization. **Geng Chen**: Writing-review & editing, Conceptualization, Investigation. **Feng Zhao**: Writing-review & editing, Supervision. **Yong Xiao**: Writing-review & editing, Writing-original draft, Conceptualization, Methodology, Supervision, Project administration, Funding acquisition.

Conflict of interests The authors declare that they have no known competing financial interests or personal relationships that could have appeared to influence the work reported in this paper.

Acknowledgements This work was supported by the National Natural Science Foundation of China (No. 22276183), the Institute of Urban Environment, Chinese Academy of Sciences (No. IUE-JBGS-202212), and the Youth Innovation Promotion Association, Chinese Academy of Sciences (No. Y2022082).

Data Availability The data that support the findings of this study are openly available in National Microbiology Data Center (NMDC) with accession number NMDC10019703 and NMDC10019704.

Electronic Supplementary material Supplementary material is available in the online version of this article at https://dx.doi.org/10.1007/s11783-025-2086-4 and is accessible for authorized users.

References

Akanuma G, Nanamiya H, Natori Y, Yano K, Suzuki S, Omata S, Ishizuka M, Sekine Y, Kawamura F (2012). Inactivation of ribosomal protein genes in *Bacillus subtilis* reveals importance of each ribosomal protein for cell proliferation and cell differentiation. Journal of Bacteriology, 194(22): 6282–6291

Alvarez A F, Georgellis D (2023). Environmental adaptation and diversification of bacterial two-component systems. Current Opinion in Microbiology, 76: 102399

Aristide L, Morlon H (2019). Understanding the effect of competition during evolutionary radiations: an integrated model of phenotypic and species diversification. Ecology Letters, 22(12): 2006–2017

Bailey S F, Dettman J R, Rainey P B, Kassen R (2013). Competition both drives and impedes diversification in a model adaptive radiation. Proceedings of the Royal Society B: Biological Sciences, 280(1766): 20131253

Barrick J E, Yu D S, Yoon S H, Jeong H, Oh T K, Schneider D, Lenski R E, Kim J F (2009). Genome evolution and adaptation in a long-term experiment with *Escherichia coli*. Nature, 461(7268): 1243–1247

Brutinel E D, Gralnick J A (2012). Preferential utilization of D-lactate by *Shewanella oneidensis*. Applied and Environmental Microbiology, 78(23): 8474–8476

Chabert N, Ali O A, Achouak W (2015). All ecosystems potentially host electrogenic bacteria. Bioelectrochemistry, 106: 88–96

Chen Y C, Dong K, Zhang Y M, Zheng J J, Jiang M M, Wang D Q, Zhang X H, Huang X W, Zhou L J, Li H X (2024). Enhancing biofilm formation in the hydrogen-based membrane biofilm reactor through bacterial Acyl-homoserine lactones. Frontiers of Environmental Science & Engineering, 18(11): 142

Demirbas A (2011). Waste management, waste resource facilities and waste conversion processes. Energy Conversion and Management, 52(2): 1280–1287

Dubuisson J F, Vianney A, Hugouvieux-Cotte-Pattat N, Lazzaroni J C (2005). Tol-Pal proteins are critical cell envelope components of *Erwinia chrysanthemi* affecting cell morphology and virulence. Microbiology, 151(10): 3337–3347

Farshadzadeh Z, Taheri B, Rahimi S, Shoja S, Pourhajibagher M, Haghighi M A, Bahador A (2018). Growth rate and biofilm formation ability of clinical and laboratory-evolved colistin-resistant strains of *Acinetobacter baumannii*. Frontiers in Microbiology, 9: 153

Finkel S E, Kolter R (1999). Evolution of microbial diversity during prolonged starvation. Proceedings of the National Academy of Sciences of the United States of America, 96(7): 4023–4027

Foster K R, Bell T (2012). Competition, not cooperation, dominates interactions among culturable microbial species. Current Biology, 22(19): 1845–1850

Ghoul M, Mitri S (2016). The ecology and evolution of microbial competition. Trends in Microbiology, 24(10): 833–845

Groisman E A (2016). Feedback control of two-component regulatory systems. Annual Review of Microbiology, 70: 103–124

Gude S, Pinçe E, Taute K M, Seinen A B, Shimizu T S, Tans S J (2020). Bacterial coexistence driven by motility and spatial competition. Nature, 578(7796): 588–592

Hale C A, de Boer P A J (1997). Direct binding of FtsZ to ZipA, an essential component of the septal ring structure that mediates cell division in *E. coli*. Cell, 88(2): 175–185

Herlihey F A, Moynihan P J, Clarke A J (2014). The essential protein for bacterial flagella formation Flgj functions as a *β-N*-acetylglucosaminidase. Journal of Biological Chemistry, 289(45): 31029–31042

Hoffmann A A, Hercus M J (2000). Environmental stress as an evolutionary force. BioScience, 50(3): 217–226

Hu L, Fang X Y, Wen L L, Zhang H X, Peng B Y, Li C C (2024). Molecular insights into the enhanced growth of cyanobacteria by adaptive laboratory evolution in wastewater environments. Algal Research, 83: 103724

Koch C, Harnisch F (2016). Is there a specific ecological niche for electroactive microorganisms? ChemElectroChem, 3(9): 1282–1295

Koch C, Korth B, Harnisch F (2018). Microbial ecology-based engineering of Microbial Electrochemical Technologies. Microbial Biotechnology, 11(1): 22–38

Kundu B B, Krishnan J, Szubin R, Patel A, Palsson B O, Zielinski D C, Ajo-Franklin C M (2025). Extracellular respiration is a latent energy metabolism in *Escherichia coli*. Cell, 188(11): 2907–2924

Lawrence D, Fiegna F, Behrends V, Bundy J G, Phillimore A B, Bell T, Barraclough T G (2012). Species interactions alter evolutionary responses to a novel environment. PLoS Biology,

10(5): e1001330

Lee S H, van der Werf J H J, Hayes B J, Goddard M E, Visscher P M (2008). Predicting unobserved phenotypes for complex traits from whole-genome SNP data. PLoS Genetics, 4(10): e1000231

Lenski R E, Travisano M (1994). Dynamics of adaptation and diversification: a 10,000-generation experiment with bacterial populations. Proceedings of the National Academy of Sciences of the United States of America, 91(15): 6808–6814

Li F H, Tang Q, Fan Y Y, Li Y, Li J, Wu J H, Luo C F, Sun H, Li W W, Yu H Q (2020). Developing a population-state decision system for intelligently reprogramming extracellular electron transfer in *Shewanella oneidensis*. Proceedings of the National Academy of Sciences of the United States of America, 117(37): 23001–23010

Li M, Ho P Y, Yao S J, Shimizu K (2006). Effect of *sucA* or *sucC* gene knockout on the metabolism in *Escherichia coli* based on gene expressions, enzyme activities, intracellular metabolite concentrations and metabolic fluxes by ^{13}C-labeling experiments. Biochemical Engineering Journal, 30(3): 286–296

Lin X H, Yang F, You L X, Wang H, Zhao F (2021). Liposoluble quinone promotes the reduction of hydrophobic mineral and extracellular electron transfer of *Shewanella oneidensis* MR-1. The Innovation, 2(2): 100104

Locey K J, Lennon J T (2016). Scaling laws predict global microbial diversity. Proceedings of the National Academy of Sciences of the United States of America, 113(21): 5970–5975

Logan B E, Hamelers B, Rozendal R, Schröder U, Keller J, Freguia S, Aelterman P, Verstraete W, Rabaey K (2006). Microbial fuel cells: methodology and technology. Environmental Science & Technology, 40(17): 5181–5192

Logan B E, Rossi R, Ragab A A, Saikaly P E (2019). Electroactive microorganisms in bioelectrochemical systems. Nature Reviews Microbiology, 17(5): 307–319

Lovley D R (1991). Dissimilatory Fe(III) and Mn(IV) reduction. Microbiological Reviews, 55(2): 259–287

MacLean R C (2008). The tragedy of the commons in microbial populations: insights from theoretical, comparative and experimental studies. Heredity, 100(5): 471–477

Martín-Rodríguez A J, Higdon S M, Thorell K, Tellgren-Roth C, Sjöling Å, Galperin M Y, Krell T, Römling U (2022). Comparative genomics of cyclic di-GMP metabolism and chemosensory pathways in *Shewanella algae* strains: novel bacterial sensory domains and functional insights into lifestyle regulation. mSystems, 7(2): e01518–21

McLean J S, Pinchuk G E, Geydebrekht O V, Bilskis C L, Zakrajsek B A, Hill E A, Saffarini D A, Romine M F, Gorby Y A, Fredrickson J K, et al. (2008). Oxygen-dependent autoaggregation in *Shewanella oneidensis* MR-1. Environmental Microbiology, 10(7): 1861–1876

Melton E D, Swanner E D, Behrens S, Schmidt C, Kappler A (2014). The interplay of microbially mediated and abiotic reactions in the biogeochemical Fe cycle. Nature Reviews Microbiology, 12(12): 797–808

Mitri S, Foster K R (2013). The genotypic view of social interactions in microbial communities. Annual Review of Genetics, 47: 247–273

Moczek A P, Hunt J, Emlen D J, Simmons L W (2002). Threshold evolution in exotic populations of a polyphenic beetle. Evolutionary Ecology Research, 4(4): 587–601

Moens S, Vanderleyden J (1996). Functions of bacterial flagella. Critical Reviews in Microbiology, 22(2): 67–100

Nakamura S, Minamino T (2019). Flagella-driven motility of bacteria. Biomolecules, 9(7): 279

Palmer J D, Foster K R (2022). Bacterial species rarely work together. Science, 376(6593): 581–582

Pettersen A K, Hall M D, White C R, Marshall D J (2020). Metabolic rate, context-dependent selection, and the competition-colonization trade-off. Evolution Letters, 4(4): 333–344

Pfeiffer T, Schuster S, Bonhoeffer S (2001). Cooperation and competition in the evolution of ATP-producing pathways. Science, 292(5516): 504–507

Pinchuk G E, Hill E A, Geydebrekht O V, De Ingeniis J, Zhang X L, Osterman A, Scott J H, Reed S B, Romine M F, Konopka A E, et al. (2010). Constraint-based model of *Shewanella oneidensis* MR-1 metabolism: a tool for data analysis and hypothesis generation. PLoS Computational Biology, 6(6): e1000822

Pinchuk G E, Rodionov D A, Yang C, Li X Q, Osterman A L, Dervyn E, Geydebrekht O V, Reed S B, Romine M F, Collart F R, et al. (2009). Genomic reconstruction of *Shewanella oneidensis* MR-1 metabolism reveals a previously uncharacterized machinery for lactate utilization. Proceedings of the National Academy of Sciences of the United States of America, 106(8): 2874–2879

Pohlschroder M, Ghosh A, Tripepi M, Albers S V (2011). Archaeal type IV pilus-like structures-evolutionarily conserved prokaryotic surface organelles. Current Opinion in Microbiology, 14(3): 357–363

Qi X Y, Cai H W, Wang X L, Liu R J, Cai T, Wang S, Liu X Y, Wang X (2024). Electricity generation by *Pseudomonas putida* B6-2 in microbial fuel cells using carboxylates and carbohydrate as substrates. Engineering Microbiology, 4(2): 100148

Rabaey K, Rodríguez J, Blackall L L, Keller J, Gross P, Batstone D, Verstraete W, Nealson K H (2007). Microbial ecology meets electrochemistry: electricity-driven and driving communities. The ISME Journal, 1(1): 9–18

Rigato E, Fusco G (2020). Effects of phenotypic robustness on adaptive evolutionary dynamics. Evolutionary Biology, 47(3): 233–239

Semmler A B T, Whitchurch C B, Leech A J, Mattick J S (2000). Identification of a novel gene, *fimV*, involved in twitching motility in *Pseudomonas aeruginosa*. Microbiology, 146(6): 1321–1332

Shen A L, Liu H Y, Zhu Y L, Zeng J N (2024). Long-term response of interspecific competition among three typical bloom-forming species to changes in phosphorus and temperature. Marine Environmental Research, 196: 106421

Shi L, Dong H L, Reguera G, Beyenal H, Lu A H, Liu J, Yu H Q, Fredrickson J K (2016). Extracellular electron transfer mechanisms between microorganisms and minerals. Nature Reviews Microbiology, 14(10): 651–662

Shimizu T, Ichimura K, Noda M (2016). The surface sensor NlpE of enterohemorrhagic *Escherichia coli* contributes to regulation of the type III secretion system and flagella by the Cpx response to adhesion. Infection and Immunity, 84(2): 537–549

Sun J F, Li X, Qiu Y, Xue X F, Zhang M M, Yang W H, Zhou D S, Hu L F, Lu R F, Zhang Y Q (2022). Quorum sensing regulates transcription of the pilin gene *mshA1* of MSHA pilus in *Vibrio parahaemolyticus*. Gene, 807: 145961

Tasteyre A, Barc M C, Collignon A, Boureau H, Karjalainen T (2001). Role of FliC and FliD flagellar proteins of *Clostridium difficile* in adherence and gut colonization. Infection and Immunity, 69(12): 7937–7940

Teleha M A, Miller A C, Larsen R A (2013). Overexpression of the *Escherichia coli* TolQ protein leads to a null-FtsN-like division phenotype. MicrobiologyOpen, 2(4): 618–632

Venkataram S, Monasky R, Sikaroodi S H, Kryazhimskiy S, Kacar B (2020). Evolutionary stalling and a limit on the power of natural selection to improve a cellular module. Proceedings of the National Academy of Sciences of the United States of America, 117(31): 18582–18590

Xiao C Y, Xiao Y, Zhao F (2019). Mechanism of long-term chromium stress on *Shewanella oneidensis* MR-1 using whole genome resequencing technique. China Environmental Science, 39(3): 1261–1267

Xiao Y, Chen G, Chen Z, Bai R, Zhao B Y, Tian X C, Wu Y C, Zhou X, Zhao F (2021). Interspecific competition by non-exoelectrogenic *Citrobacter freundii* An1 boosts bioelectricity generation of exoelectrogenic *Shewanella oneidensis* MR-1. Biosensors and Bioelectronics, 194: 113614

Yan X J, Du Q, Mu Q H, Tian L L, Wan Y X, Liao C M, Zhou L A, Yan Y Q, Li N, Logan B E, et al. (2021). Long-term succession shows interspecies competition of *Geobacter* in exoelectrogenic biofilms. Environmental Science & Technology, 55(21): 14928–14937

Yang C H, Aslan H, Zhang P, Zhu S J, Xiao Y, Chen L X, Khan N, Boesen T, Wang Y L, Liu Y, et al. (2020). Carbon dots-fed *Shewanella oneidensis* MR-1 for bioelectricity enhancement. Nature Communications, 11(1): 1379

Yang F, Li J P, Wang H, Xiao X F, Bai R, Zhao F (2023). Visible light induces bacteria to produce superoxide for manganese oxidation. Frontiers of Environmental Science & Engineering, 17(2): 19

Yin J H, Meng Q, Fu H H, Gao H C (2016). Reduced expression of cytochrome oxidases largely explains cAMP inhibition of aerobic growth in *Shewanella oneidensis*. Scientific Reports, 6: 24449

Yu Y, Ndayisenga F, Yu Z S, Zhao M Y, Lay C H, Zhou D D (2019). Co-substrate strategy for improved power production and chlorophenol degradation in a microbial fuel cell. International Journal of Hydrogen Energy, 44(36): 20312–20322

Zaidi S, Hassan M I, Islam A, Ahmad F (2014). The role of key residues in structure, function, and stability of cytochrome-*c*. Cellular and Molecular Life Sciences, 71(2): 229–255

Zhang Z J, van Kleunen M, Becks L, Thakur M P (2020). Towards a general understanding of bacterial interactions. Trends in Microbiology, 28(10): 783–785

Zheng Y, Wang H, Liu Y, Zhu B L, Li J H, Yang Y Y, Qin W, Chen L F, Wu X E, Chistoserdova L, et al. (2020). Methane-dependent mineral reduction by aerobic methanotrophs under hypoxia. Environmental Science & Technology Letters, 7(8): 606–612

Zöllner R, Oldewurtel E R, Kouzel N, Maier B (2017). Phase and antigenic variation govern competition dynamics through positioning in bacterial colonies. Scientific Reports, 7(1): 12151